

Ab initio molecular dynamics simulations of β -D-glucose and β -D-xylose degradation mechanisms in acidic aqueous solution

Xianghong Qian,^{a,*} Mark R. Nimlos,^b Mark Davis,^b
David K. Johnson^b and Michael E. Himmel^b

^a*Rx-Innovation, Inc., Fort Collins, CO 80525, USA*

^b*National Bioenergy Center, National Renewable Energy Laboratory, Golden, CO 80401, USA*

Received 22 February 2005; accepted 11 July 2005

Available online 10 August 2005

Abstract—Ab initio molecular dynamics simulations were employed to investigate, with explicit solvent water molecules, β -D-glucose and β -D-xylose degradation mechanisms in acidic media. The rate-limiting step in sugar degradation was found to be protonation of the hydroxyl groups on the sugar ring. We found that the structure of water molecules plays a significant role in the acidic sugar degradation pathways. Firstly, a water molecule competes with the hydroxyl group on the sugar ring for protons. Secondly, water forms hydrogen bonds with the hydroxyl groups on the sugar rings, thus weakening the C–C and C–O bonds (each to a different degree). Note that the reaction pathways could be altered due to the change of relative stability of the C–C and C–O bonds. Thirdly, water molecules that are hydrogen-bonded to sugar hydroxyls could easily extract a proton from the reaction intermediate, terminating the reaction. Indeed, the sugar degradation pathway is complex due to multiple protonation probabilities and the surrounding water structure. Our experimental data support multiple sugar acidic degradation pathways.

© 2005 Elsevier Ltd. All rights reserved.

Keywords: β -D-Glucose; β -D-Xylose; Degradation; Pathway; Acidic; Water structure

1. Introduction

To prepare lignocellulosic biomass for cellulase digestion, dilute acid treatments are commonly used to hydrolyze hemicellulose to soluble xylooligosaccharides and β -D-xylose. If the severity of the pretreatment process is sufficiently high, a portion of the cellulose may also be hydrolyzed to β -D-glucose.¹ Even though the cost of cellulase enzymes for cellulose hydrolysis to fermentable sugars has been reduced dramatically in recent years, and enzymatic conversion demonstrates a clear advantage, dilute acid-mediated hydrolysis remains a viable option.² The loss of fermentable sugars to acidic degradation is one potential cause of low feedstock yield and high processing cost for lignocellulosic biomass conversion. The decreased yield of β -D-glucose and

β -D-xylose during prehydrolysis could significantly affect the economic viability of these processes.^{1,3} In addition, sugar degradation products such as furfural and hydroxymethylfurfural (HMF) could inhibit enzymatic action and sugar fermentation.⁴

In order to improve sugar yield and reduce degradation products, particularly during dilute acid pretreatment and hydrolysis, understanding sugar degradation pathways at the molecular level is critical. In the past, sugar yield and acidic sugar degradation products were found to be strongly dependent upon the reactor configuration, the reaction media, and the reaction temperature.^{5–8} Furthermore, a flow-through percolation reactor reported by Torget and co-workers increased cellulose conversion and glucose yield significantly compared to a batch reactor.⁵ It was also reported that acidity (i.e., pH) and temperature could affect glucose yield dramatically.^{6–8} In addition, glucose yield for a pretreated yellow poplar increased from 42% to 55%

* Corresponding author. E-mail: xianghong_qian@nrel.gov

theoretical yield without ethanol, to 85% yield with 0.2 wt. % ethanol added to the reaction media during dilute (0.07 wt. %) sulfuric acid hydrolysis at 498 K.⁹

To complicate matters further, it was commonly thought that furfural and HMF are by far the principal acidic degradation products for β -D-glucose and β -D-xylose, respectively. However, experimentally observed furfural and HMF production account for only a portion of the sugar loss observed during pretreatment.^{5–8,10} For xylose degradation in acidic medium at an elevated temperature (525 K), at least 10 different degradation products besides furfural were identified, including formaldehyde, formic acid, acetaldehyde, crotonaldehyde, lactic acid, dihydroxyacetone, glyceraldehydes, pyruvaldehyde, acetol, and glycolaldehyde.¹¹ Some parasitic degradation pathways leading to the formation of noncellulosic polymeric materials have also been suggested for glucose degradation.^{10,12} The detailed mechanisms for these reactions are not currently known. For furfural and HMF formation, some researchers^{12,13} have proposed degradation pathways that proceed via a series of open-chain intermediates. In contrast, Antal and co-workers¹¹ have proposed a mechanism based on a 2,5-anhydride intermediate for xylose degradation leading to furfural. Nevertheless, the precise mechanism for the formation of furfural and HMF remains an open question. Moreover, it was observed experimentally that β -D-xylose degrades much faster than β -D-glucose.⁹ Since these structures are very similar to each other, it is puzzling why their reactivities are so different. In order to optimize pretreatment conditions to maximize sugar yield, it will be of tremendous value to understand more deeply how the reaction media and conditions affect β -D-xylose and β -D-glucose yields. Ab initio molecular dynamics (MD) simulation provides an ideal tool for this study.

Previously, we reported acidic β -D-glucose and β -D-xylose degradation mechanisms without considering the reaction media effect.¹⁴ Because there are five and four hydroxyl groups on the β -D-glucose and β -D-xylose molecules, respectively (shown in Fig. 1), all probable protonation scenarios of these hydroxyl groups and the ring oxygen were examined. It was found that the carbon cation, formed after the protonated –OH group (i.e., H₂O) leaves the ring, could rearrange to form degradation products depending on its stability. We found that protonation of the 2-OH on β -D-glucose and β -D-xylose, which leads to the formation of HMF and furfural, respectively, via carbon cation rearrangement, was in agreement with the mechanisms proposed earlier by Antal and co-workers.¹¹ In the case of glucose, protonations of 3-OH and 4-OH lead to two different five-membered ring degradation products other than HMF, which may account for the other noncellulosic materials observed experimentally.¹⁰ Protonations of 1-OH and 6-OH did not lead to any observable reaction.

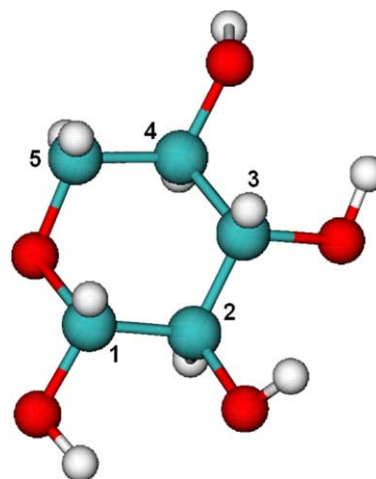


Figure 1. The atomic structure of a β -D-xylose. Each hydroxyl group on the sugar ring is numbered counterclockwise according to its relative location to the ring O.

Protonation of the ring oxygen was found to lead to equilibrium between the open- and closed-ring structures. In the case of β -D-xylose, protonation of the 3-OH leads to the opening of the ring structure and the fragmentation of β -D-xylose into C₁ and C₄ products, which were observed experimentally.¹¹ Protonations of 1-OH and 4-OH did not lead to any carbon cation rearrangement in our simulations. The reactivity of these sugar molecules is considered dependent on the stability of the carbon cation after the protonated –OH group leaves the ring, because in this case protonation is already assumed. From the simulations in vacuum, β -D-glucose was found to be slightly more reactive than β -D-xylose, which is contrary to what was observed experimentally.⁹ Our calculations indicated that the charges on the ring carbon atoms in β -D-glucose are slightly more positive than those in β -D-xylose, which makes the glucose carbon cation more prone to rearrangement than the xylose carbon cation. This discrepancy between experimental observation and simulation results could be accounted for by the solvent effect, which was not included in our earlier simulations.

In the present study, the effects of reaction media with explicit water molecules were investigated using ab initio MD simulations. Protonation of the hydroxyl groups on the sugar rings was found to be the rate-limiting step for sugar degradation in dilute acid environment. From our simulation results, it appears that competition for protons among various weaker bases, such as H₂O, the ring-O, the sugar ring hydroxyl groups, and cosolvents such as ethanol, is one of the main reasons why sugar yield is media dependent. In addition, the simulation results show that hydrogen-bonding (HB) interactions between the solvent water molecule and –OH groups on the sugar ring could alter the reaction pathway by upsetting the relative stability of the C–C and C–O

bonds on the sugar ring. These hydrogen-bonded water molecules could also easily extract a proton from one of the reaction intermediate, thus terminating the ring closure reaction. The effects of pH on sugar yields and degradation pathways will be discussed.

2. Experimental

2.1. Computational methods

Ab initio MD simulations based on Car–Parrinello (CPMD) approach¹⁵ were employed in this study.¹⁶ CPMD combines density-functional theory (DFT) with molecular dynamics approach. The core electrons are frozen during the simulations since they contribute very little to the inter-atomic potential. The valence and semi-core electrons are treated quantum mechanically. The nuclei are treated classically without accounting for the quantum effect. Each β -D-glucose and β -D-xylose in our simulation was surrounded by 32 water molecules in a unit cell with a lattice parameter of 11.5 Å. Each glucose and xylose molecule had approximately two hydration shells. In addition, one proton was added to the system to mimic the acidic medium. Periodic boundary conditions were applied. The simulated water density was lower than bulk water because water density is expected to vary with solute concentrations and reaction conditions. Our goal was to investigate the role of solvent water molecules in xylose and glucose degradation rather than to mimic actual reaction conditions. Further studies will be carried out with realistic reaction conditions, which are far more complex than this simulation due to the presence of salts and other cosolvents. An electron mass of 800 a.u. and a time-step of 0.125 fs (femtosecond) were used in these calculations. The simulation timescale did not correspond exactly to the real timescale, but close. The Becke, Lee, Yang, and Parr (BLYP) gradient corrected functional^{17,18} was used, which was shown to be appropriate to describe the liquid water.^{19,20} The valence and semi-core electrons were treated with Troullier–Martin norm-conserving pseudopotential.²¹ Only the energy at the Γ -point was calculated. The plane-wave basis set cut-off was 70 Ry, which was shown to be sufficient for biomolecular simulations in aqueous solution.²⁰ Ab initio MD was carried out at a constant temperature of 500 K, which was at the higher end of the pretreatment temperature, but was close to the most experimental temperatures cited here. Temperature effects will be the subject of our future investigations.

2.2. Hydrolytic experimental procedures

Cellulose hydrolyses were performed in small glass batch reactors using dilute sulfuric acid (0.07 wt. %), at temperatures in the range of 478–493 K, reaction times

of 15–120 min, and with J. T. Baker cellulose. The hydrolysis residues were analyzed to permit assessment of the degree of cellulose conversion and the amount of noncellulosic material present in the residue. High-resolution, solid-state ^{13}C NMR spectra were collected at 4.7 T with cross-polarization (CP) and magic angle spinning (MAS) in a Bruker Avance 200 MHz spectrometer. Spectra were obtained from a series of solid residues collected after the acid hydrolysis of J. T. Baker cellulose. Solid-state ^{13}C CP/MAS spectroscopy was not quantitative due to differences in cross polarization rates and rotating frame relaxation times. However, differences observed in relative peak intensities and integrated areas were used to identify differences between similar samples.

A series of experiments were performed in which ^{13}C -labeled and unlabeled glucose was added to the cellulose hydrolysis reactions. The conditions chosen to hydrolyze J. T. Baker cellulose with 0.07% H_2SO_4 were 205 °C for 60 min. These conditions have been shown to consistently give 92% glucan conversion. The amount of glucose added was about 10% of the weight of the cellulose in each experiment.

3. Results and discussion

3.1. Proton affinity and the rate-limiting step

Similar to the simulations carried out in vacuum,¹⁴ ab initio MD simulations started when a protonated β -D-xylose or β -D-glucose molecule was positioned in a unit cell surrounded by 32 water molecules. During the course of our entire simulation (~ 5 ps), the initiation proton attached to the –OH groups on the sugar ring was observed to be transferred back to the water molecule (Fig. 2). This transfer is rapid and occurs in less than 100 fs for all of the hydroxyl groups on the xylose ring. Once the proton was transferred to the neighboring water molecule, it is quickly transferred to other water molecules and away from the sugar molecule. This result shows that protonation is probably the rate-limiting step in sugar degradation under acidic media because our earlier simulations in vacuum demonstrate that protonated β -D-xylose and β -D-glucose molecules decompose rapidly. In fact, our simulation in water was only successful after separating the protonated –OH group from the sugar ring more than 2 Å, which we will discuss in more detail later. Since the proton has a very high quantum tunneling effect due to its light mass, proton transfer may be very rapid at relatively low temperature. Since our MD simulation treats nuclei classically, this effect was not taken into account in our current results. However, this quantum tunneling effect diminishes rapidly as temperature increases. At 500 K, this effect is likely to be negligible.

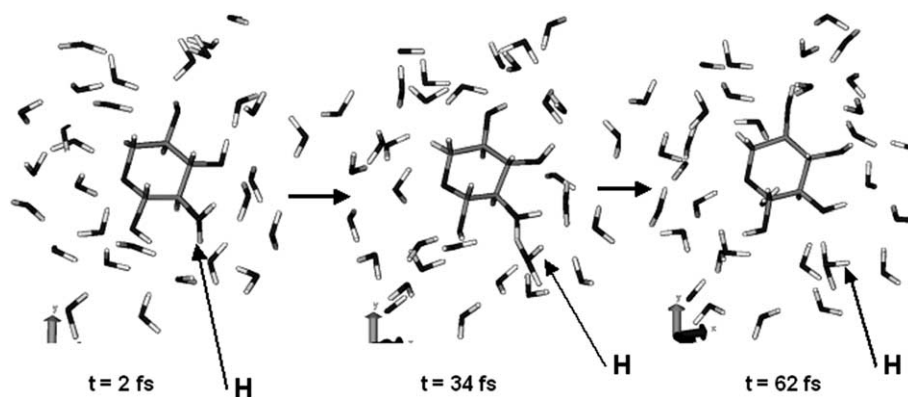


Figure 2. The left figure shows a 2-OH protonated β -D-xylose molecule surround by 32 water molecules at the start of the simulation. After less than 100 fs, the proton was seen transferred back to the solvent water molecule as shown in the right figure.

In order to support the notion that protonation is the rate-limiting step, reaction barriers have been estimated using the *ab initio* GAUSSIAN03²² program with a hybridized density functional theory B3LYP.^{17,18} For xylose degradation initiated at 2-OH in vacuum, the reaction barrier due to the breaking of the protonated –OH group and the C atom on the sugar ring to form a carbon cation intermediate is determined to be 16.9 kcal/mol. Subsequent barriers for carbon cation rearrangement and dehydration to form furfural are around 15 kcal/mol. The experimentally determined xylose degradation reaction barrier for furfural formation is about 32 kcal/mol,²³ which is significantly higher than the barrier found in vacuum. That is to say, this reaction barrier is much higher due to the presence of solvent water molecules. Additional calculations were carried out with one to four water-molecule clusters surrounding the 2-OH group of the xylose molecule. The reaction barriers are found to be in the range between 30 and 41 kcal/mol, depending on the number of water molecules. The agreement with the experimentally determined barrier is much closer compared to the case without explicit solvent water molecules. Water molecules clearly play an important role in sugar degradation due to their higher proton affinity compared to xylose.

Since the solvent water is a weak base, it will compete with the –OH groups on the sugar ring for proton. It also appears that water has a higher proton affinity compared to the hydroxyl groups on the sugar ring. Compared to other alcohols, such as ethanol and propanol, the proton affinities of β -D-xylose and β -D-glucose are quite different. We also carried out simulations for protonated ethanol and propanol in water (not shown here), and it appears that these alcohols have a higher proton affinity compared to that of water. In the prehydrolysis reaction media where there are a number of weak bases in solution, including the hydroxyl groups on the sugar molecule, the ring oxygen, the β -(1 \rightarrow 4)-linkage between the monomer sugar molecules in xylan and cellulose, and possibly other cosolvent and salts.

Our results indicate that there are competitions for protons among these various weak bases at lower proton concentrations. This is perhaps why adding a small amount of ethanol in earlier experiments could increase glucose yield dramatically.⁹ For example, as ethanol absorbed available protons, β -D-xylose and β -D-glucose molecules would be shielded from proton attack. In this case, the effective acidity surrounding the sugar molecules in solution becomes lower. Understanding the rate-limiting step in sugar degradation mechanisms also explains why degradation pathway and products could be reaction media and condition dependent.^{5–9}

In our earlier vacuum simulations,¹⁴ we have shown that multiple degradation pathways are possible due to protonations initiated at 2-, 3-, and 4-OH on glucose and 2- and 3-OH on xylose. Because these –OH groups have different chemical environments, their proton affinities are probably different. Indeed, the NMR data^{24–26} show that all these –OH groups are downshifted with respect to water. Furthermore, the shifts are different for these –OH groups at different positions with $\text{H}_2\text{O} > 6\text{-OH} > 2\text{-OH} > 3,4\text{-OH} > 1\text{-OH}$. In addition, our earlier results¹⁴ show that protonations of 6-OH and the ring-O do not lead to observed degradation during the simulation period; therefore, the most likely β -D-xylose and β -D-glucose degradation pathways will be initiated at the 2-OH at lower acidity because it has a higher proton affinity than the other hydroxyl groups on the sugar ring. Our earlier simulations¹⁴ confirm that protonations initiated at 2-OH lead to the primary observed degradation products, HMF and furfural. However, at higher acidity where protonation may not be the rate-limiting step, degradation initiated at 3-, 4-OH is also possible, thus leading to multiple degradation products as was observed experimentally.¹⁰

3.2. The effect of water on glucose degradation pathways

Since protonation of the hydroxyl groups on the sugar ring is likely to be the rate-limiting step in very dilute

acidic media, our simulations of β -D-glucose degradation in water with a protonated hydroxyl group on the sugar ring did not lead to observed glucose degradation because the proton was readily transferred back to the solvent water molecule. In order to facilitate the glucose degradation, we initially separated the protonated $-OH$ group (i.e., H_2O) from the sugar ring at a distance of more than 2 Å. The *ab initio* MD simulation started from there. Again, all probable protonations of all the $-OH$ group on the sugar ring were investigated.

Figure 3 shows the β -D-glucose degradation pathway initiated from 2-OH in aqueous solution with 32 water molecules and a single proton. Water molecules have been removed in the figure in order to illustrate the pathways more clearly (only the water molecules involved in the reaction were retained). The reaction mechanism observed here is very similar to the one in vacuum, except that a solvent water molecule was implicated in the reaction. The carbon cation arrangement occurs rapidly after the protonated $-OH$ group was separated from the carbon ring. Indeed, it confirms our previous observation that protonation is the rate-limiting step. Since water is hydrogen bonded to the hydroxyl group on the sugar ring, water molecules could easily extract a proton from the $-C^+-OH$ to form $-C=O$, thus neutralizing the sugar molecule and terminating the reaction.

Figure 4 exhibits the β -D-glucose degradation pathway initiated at the 3-OH. From this figure, it can be seen that the reaction in water is drastically different from that in vacuum.¹⁴ In vacuum, the rearrangement of the carbon cation after the departure of the protonated hydroxyl group leads to the formation of a five-membered ring, which could polymerize to form other noncellulosic materials, including those observed experimentally.¹⁰ With explicit water, the C-1–C-2 carbon–

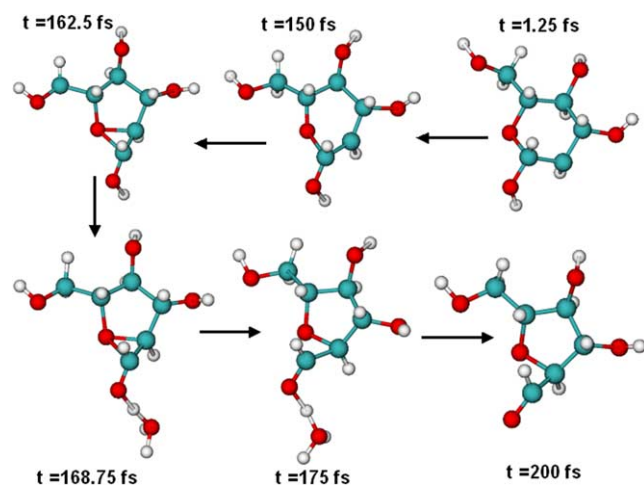


Figure 3. The reaction pathway for β -D-glucose degradation initiated at 2-OH surrounded by 32 water molecules. A HMF precursor was formed in less than 200 fs. Solvent water molecules, except one involved in the reaction were removed from the figure in order to illustrate the pathway more clearly.

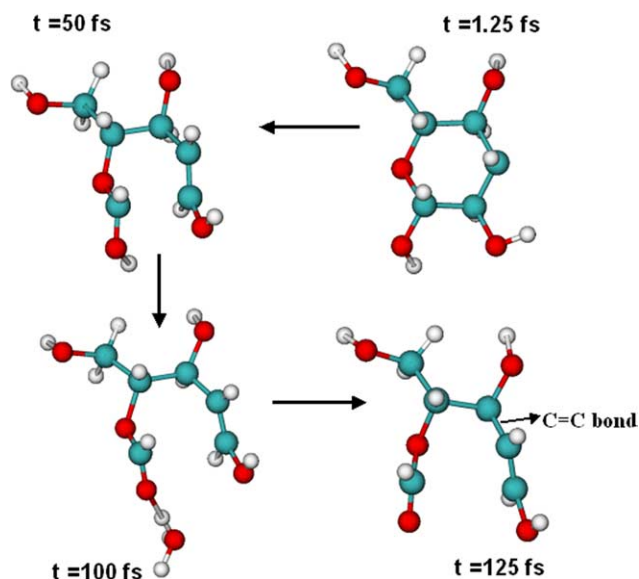


Figure 4. Reaction pathway for β -D-glucose degradation initiated at 3-OH surrounded by 32 water molecules. Solvent water molecules except one involved in reaction were removed in the figure. Water terminates the ring closure reaction by extracting a proton from an intermediate.

carbon bond was elongated and eventually broken after the formation of $-C-3^+$ carbon cation. Due to the presence of the 1-OH hydrogen bonded water molecule, a proton was extracted to form the CHO end group. A $C=C$ double bond was also formed between the C-2 (anion) and C-3 (cation) carbon atoms, thus eliminating the possibility of five-membered ring closure. Figure 4 shows that water structure plays a significant role in sugar degradation pathways due to hydrogen-bonding interaction between water and the sugar molecules. Water readily accepts and donates a proton depending on the specific reaction conditions. Since the proton affinity of the 3-OH is relatively lower compared to the 2-OH in glucose, glucose decomposition initiated at 3-OH will only occur at a relatively higher acidity. Thus this reaction mechanism may or may not be observed experimentally based on reaction conditions.

Figure 5 shows glucose degradation in aqueous solution initiated by protonation at 4-OH after the protonated $-OH$ was separated from the carbon ring. Once again we observed that decomposition is rapid on a time scale less than 1 ps. Sugar hydroxyl–hydrogen-bonded solvent water molecules extract a proton from one of the reaction intermediates and terminate the ring-closure reaction (which was observed in vacuum). Due to the participation of water in these reactions, water structure is crucial for steering the sugar degradation pathways. Water structure is in turn determined by the pH of the reaction media, temperature, the presence of cosolvents, and salts in solution. This is perhaps why experimentally observed sugar decomposition products are strongly dependent on reaction conditions. In addition, dynamic conditions existing in a reactor, such as

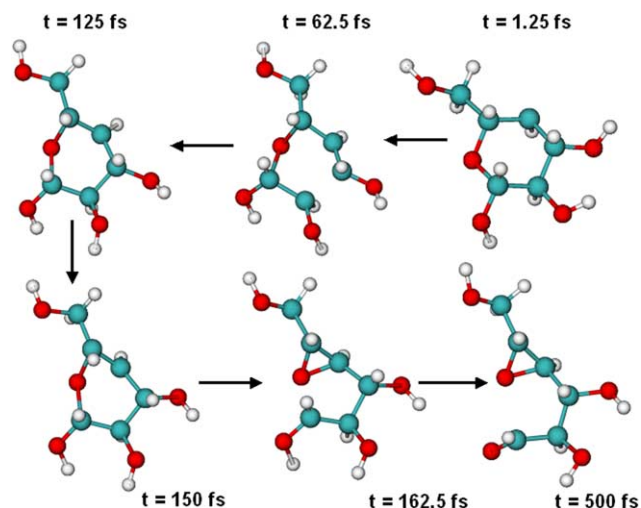


Figure 5. Reaction pathway for β -D-glucose decomposition initiated at 4-OH in aqueous solution. Solvent water molecules were removed in the figure in order to illustrate the reaction pathway more clearly.

flow, will also influence not only the water structure, but also the conformation of the sugar molecules and the hydrogen-bonding interaction between water and sugars. Nevertheless, the most important step in sugar degradation is the protonation of the sugar molecule, which depends on the proton affinity and competition among various weak bases in solution. Since the pH and water structure here do not represent the real pretreatment condition, β -D-glucose degradation in an actual reactor will not necessarily follow the degradation pathway found here.

As with the vacuum case, protonations of 6-OH and the ring oxygen do not lead to observable decomposition of the glucose molecule. Also, the opening of the ring structure via protonation of the ring oxygen, which is actually the first step in mutarotation to reach the anomeric equilibrium (i.e., α - and β -glucose mixture) in solution, was confirmed experimentally.²⁷ This process occurs slowly and is on the time scale of several hours in pure water at room temperature. But this reaction could probably be catalyzed with an acid.

3.3. Experimental evidence for multiple degradation pathways

Figure 6 shows ^{13}C NMR spectra for the solid residue collected after the acid hydrolysis of J. T. Baker cellulose after 92% of the sample was converted to products. The peak assignments are shown according to earlier studies.^{28,29} The peak at ~ 105 ppm is assigned to the C-1 carbon of the cellulose and the hemicelluloses. The peaks at 89 and 66 ppm are assigned to the C-4 and C-6 carbons, respectively, found in crystalline environments (cellulose), whereas the peaks at 84 and 60 ppm are assigned to the C-4 and C-6 carbons, respectively, in amorphous regions (cellulose and hemicellulose).

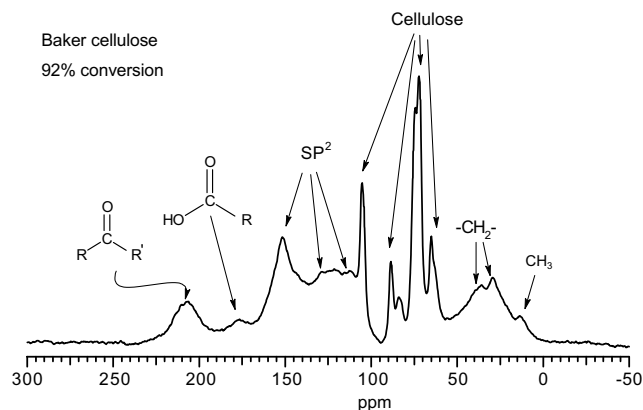


Figure 6. Peak assignments for ^{13}C CP/MAS spectra of J. T. Baker cellulose after acid hydrolysis for 60 min.

The peaks at ~ 72 ppm are assigned to C-2, C-3, and C-5. The spectrum indicates the polymeric material consists of carbonyl carbons (aldehydes, ketones, or carboxylic acids, 160–210 ppm), aromatic, or olefinic sp^2 carbons (110–160 ppm), methylene carbons (20–30 ppm), and methyl carbons (~ 13 ppm).

The difference spectra of the residues, shown in Figure 7, prepared with the ^{13}C -labeled glucose, indicate that several different pathways are present in the formation of the solid residue. The difference spectra were prepared by subtracting the spectrum of the residue prepared with the unlabeled glucose (spectrum not shown, but almost identical to the 92% conversion spectrum shown in Fig. 6) from the spectra of the labeled residues. The intensity of the peaks from the residual cellulose was used as an internal standard and the subtractions were performed to minimize intensity in this region. The spectrum of the residue prepared using the added C-1-labeled glucose shows that a large fraction of the labeled glucose was converted into sp^2 carbons with smaller amounts converted into carbonyls and sp^3 carbons. The peak at 178 ppm, possibly unreacted aldehyde side groups, is also indicative of HMF being incorporated into the polymer. The peak at 206 ppm, assigned to a ketone carbonyl, and the peaks at 144 and 124 ppm, assigned to sp^2 carbons of unknown origin, may be due to alternative pathways of glucose degradation. The C-2 carbon appears to be incorporated into the polymer in three chemically similar sites. The peaks at 141 ppm assigned to sp^2 carbons of unknown origin and 206 ppm, assigned to a ketone carbonyl, again suggest alternative pathways such as glucose dehydration that does not lead to HMF.

3.4. The effect of water on β -D-xylose degradation pathways

Similar to β -D-glucose degradation, β -D-xylose degradation in acidic aqueous solution is also strongly affected

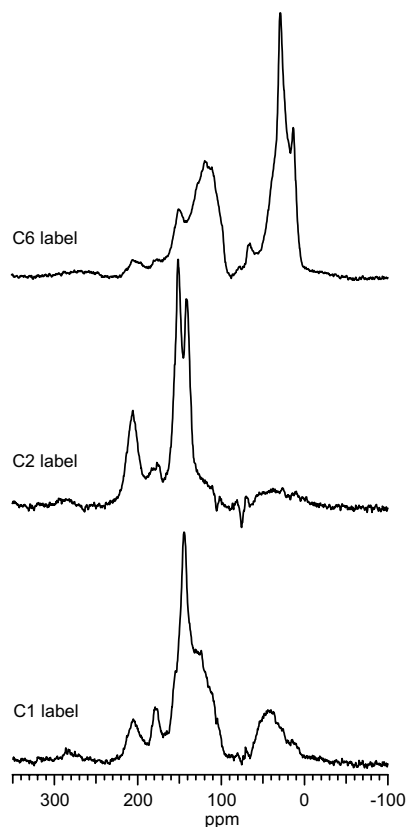


Figure 7. Difference spectra of residues obtained after the addition of ^{13}C -labeled glucose. The spectra were derived by subtracting the spectrum of the residue obtained after the addition of unlabeled glucose from the spectra obtained after addition of labeled glucose. The difference spectra only show intensity due to the specific labeled carbon.

by the reaction conditions. Figures 8–10 show β -D-xylose degradation pathways under similar conditions to β -D-glucose. Xylose decomposition was initiated by protonations of 2-OH and 3-OH. Protonations of 1-OH and 4-OH do not seem to lead to xylose degradation. For these simulations, each unit cell consists of a β -D-xylose molecule surrounded by 32 water molecules with periodic boundary condition. The protonated hydroxyl group (OH_2^+) was separated from the sugar ring to a sufficiently large distance ($>2 \text{ \AA}$) in order to initiate a carbon cation rearrangement reaction. We observed that the reaction occurred rapidly and that the protonation step is most likely the slower and thus rate-limiting step. Water structure was again seen to play an important role in these specific xylose degradation pathways.

From sugar degradation studies in vacuum, one of the intermediate steps in sugar degradation is the breaking of the C–C or C–O bond and the formation of a new C–C or C–O bond. Since the bonding energies for C–C and C–O single bonds are 348 and 360 kJ/mol, respectively,³⁰ it is possible to break either one of the

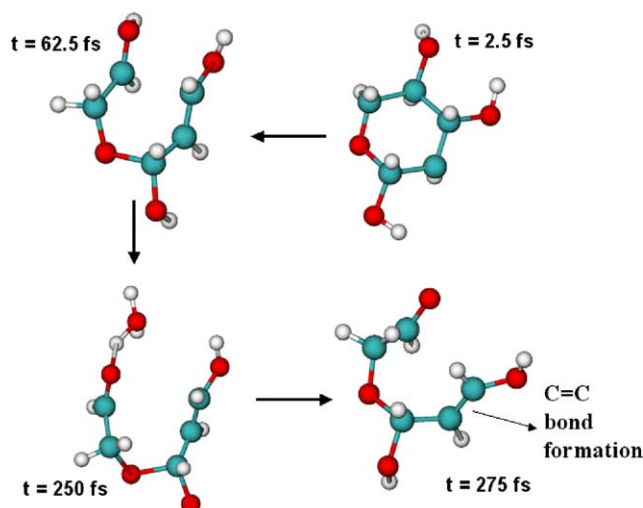


Figure 8. Reaction pathway for β -D-xylose degradation initiated at 2-OH surrounded by 32 water molecules. Solvent water molecules were removed in the figures in order to illustrate the pathway more clearly.

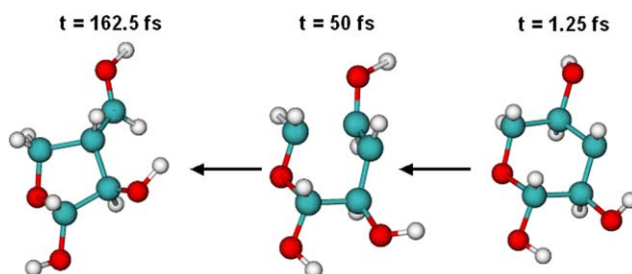


Figure 9. Reaction pathway for β -D-xylose degradation initiated at 3-OH surrounded by 32 water molecules. Reaction pathway is different from the one in vacuum. Solvent water molecules were not shown.

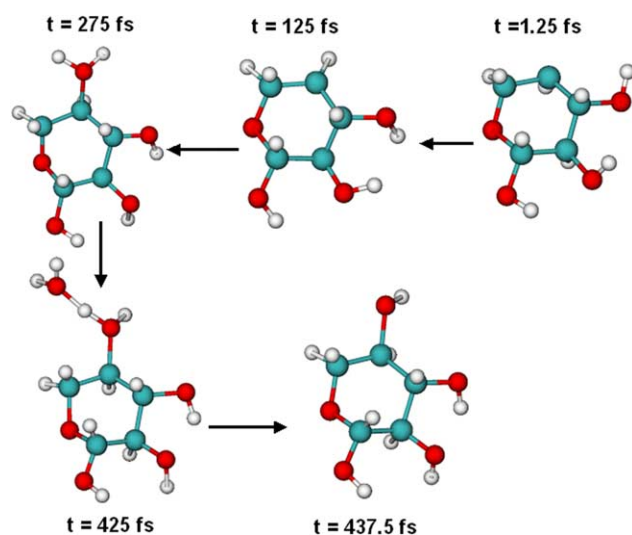


Figure 10. β -D-xylose recovery after protonated 4-OH was separated from the carbon ring. One water molecule attaches to the C-4^+ carbon cation, another water molecule extracts one proton from $\text{C-4}^+-\text{OH}_2$ to form 4-OH.

bonds, because these two energies are very close to each other. Additional complexity arises from intra-molecule and inter-molecular hydrogen-bonding interactions, thus possibly weakening the C–C and C–O bonds each to a different degree. Since hydrogen-bonding energy is around 20 kJ/mol, depending on bond angle and bond length, it could upset the relative stability of C–C and C–O bonds, thus altering the reaction pathways.

Figure 8 shows β -D-xylose degradation pathways initiated at 2-OH. Under current solvent conditions, the C-3–C-4 carbon–carbon bonds break after the protonated hydroxyl group was separated from the carbon ring. In previous β -D-xylose degradation simulations carried out in vacuum, the C-1–O-5 bond breaks after protonation of 2-OH. As a result of the hydrogen-bonding interaction between the hydroxyl groups and water under the current conditions, the C-3–C-4 bond becomes weaker than the C-1–O-5 bond. After the opening of the ring structure, water extracts a proton from the C-4⁺-OH to form –CHO. The C-3 and C-2 carbon atoms form a double bond, thus eliminating the possibility of ring closure. In this case, the xylose 2-OH protonation does not lead to the formation of furfural, in contrast to the case in vacuum where furfural was formed after 2-OH protonation. The probable explanation is due to the artificial water structure adopted here without considering the actual reactor conditions. In a different water structure, 2-OH protonation could possibly lead to furfural. More studies will be conducted on the effect of water structure.

Figure 9 shows β -D-xylose degradation after the 3-OH protonated hydroxyl group was separated from the sugar ring. This reaction mechanism is also quite different from the one observed in vacuum. After the formation of C-3⁺ carbon cation, C-4–C-5 carbon–carbon bond breaks in the current water structure while C-1–C-2 carbon–carbon bond breaks in vacuum. In less than 200 fs, a five-membered ring is formed after the closure of the C-5–C-3 bond leaving the carbon cation outside the ring.

Figure 10 shows the creation of C-4⁺ carbon cation and the subsequent reactions in aqueous solution. Without water, it was observed that protonation of 4-OH did not lead to any observable degradation of β -D-xylose. It appears that the C-4⁺ carbon cation is more stable than the C-2⁺ and C-3⁺ cations. Under aqueous conditions, it was also observed that the C-4⁺ remains very stable, and again no degradation was seen. However, due to the presence of solvent water molecules, one water molecule attaches to the C-4⁺ cation after about 200 fs. Another water molecule extracts a proton from C-4⁺-OH₂, and an intact xylose molecule is formed. For both β -D-xylose and β -D-glucose in aqueous solutions, 1-OH protonation in water does not lead to any observable degradation.

4. Conclusions

From our simulation results and experimental data, it can be seen that β -D-glucose and β -D-glucose degradation pathways in acid are likely to be strongly dependent on the water structures of the reaction media. Solvent water molecules compete with the hydroxyl groups on the sugar ring for protons. In addition, water molecules hydrogen bond with the hydroxyl groups on the sugar rings, thus weakening the C–C and C–O bonds (each to a different degree). As a result, reaction pathways could be altered due to the change of relative stability of the C–C and C–O bonds. Furthermore, water molecules that are hydrogen bonded to sugar hydroxyls could easily extract or donate a proton from/to the reaction intermediate, thus terminating the reaction. From our simulations, it can be shown that there exist different degradation products initiated at different hydroxyl groups on the sugar ring, and these products are dependent on the reaction conditions, such as temperature, pH and water structure. Our experimental NMR spectra confirm that there are multiple degradation pathways. Since proton NMR shifts of the hydroxyl groups on the sugar ring are different, we infer that each of the sugar ring hydroxyl groups have different proton affinities and reactivities. In addition, the hydroxyl that is most prone to protonation will probably be the starting position for sugar degradation.

Acknowledgements

The authors acknowledge helpful discussions with Robert Torget and Melvin Tucker at the National Renewable Energy Laboratory and John Brady at Cornell University. This work was carried out at the National Center for Supercomputers Allocation (NCSA) and Computational Science Center at NREL. Funding for this work was from the Office of Biomass Program, Department of Energy via a subcontract from the National Renewable Energy Laboratory #ACO-4-33101-01.

References

1. Wyman, C. E.; Bain, R. L.; Hinman, N. D.; Stevens, D. J. *Renewable Energy: Sources for Fuels and Electricity*; Island Press: Washington, DC, 1993.
2. Sheehan, J. J.; Himmel, M. E. *Biotechnol. Prog.* **1999**, *15*, 817–827.
3. Sheehan, J. J. In *Enzymatic Conversion of Biomass for Fuels Production*; Himmel, M. E., Baker, J. O., Overend, R. P., Eds.; American Chemical Society: Washington, DC, 1994; Vol. 566, pp 1–52.
4. Bergeron, P. In *Handbook on Bioethanol*; Wyman, C. E., Ed.; Taylor & Francis: Washington, DC, 1996, pp 179–195.
5. Torget, R. W.; Kim, J. S.; Lee, Y. Y. *Ind. Eng. Chem. Res.* **2000**, *39*, 2817–2825.

6. Kim, J. S.; Lee, Y. Y.; Torget, R. W. *Appl. Biochem. Biotechnol.* **2001**, 91–93, 331–340.
7. Xiang, Q.; Kim, J. S.; Lee, Y. Y. *Appl. Biochem. Biotechnol.* **2003**, 105–108, 337–352.
8. Xiang, Q.; Lee, Y. Y.; Torget, R. W. *Appl. Biochem. Biotechnol.* **2004**, 113–116, 1127–1138.
9. Torget R. W. Unpublished results.
10. Abatzoglou, N.; Bouchard, J.; Chornet, E.; Overend, R. P. *Can. J. Chem. Eng.* **1986**, 64, 781–786.
11. Antal, M. J.; Leesomboon, T.; Mok, W. S.; Richards, G. N. *Carbohydr. Res.* **1991**, 217, 71–85; Antal, M. J.; Mok, W. S.; Richards, G. N. *Carbohydr. Res.* **1990**, 199, 91–109; Antal, M. J.; Mok, W. S.; Richards, G. N. *Carbohydr. Res.* **1990**, 199, 111–115.
12. Garrett, E. R.; Dvorchik, B. H. *J. Pharm. Sci.* **1969**, 58, 813–820.
13. Parker, S.; Calnon, M.; Feinberg, D.; Power, A.; Weiss, C. *The Value of Furfural/Ethanol Coproduction from Acid Hydrolysis Process, SERI/TR-231-2000*; Solar Energy Research Institute: Golden, CO, 2000.
14. Qian, X.; Nimlos, M. R.; Johnson, D. K.; Himmel, M. E. *Appl. Biochem. Biotechnol.* **2005**, 121–124, 989–997.
15. Car, R.; Parrinello, M. *Phys. Rev. Lett.* **1985**, 55, 2471–2474.
16. CPMD3.7. Copyrighted jointly by IBM Corp and by Max-Planck Institute, Stuttgart; <http://www.cpmid.org>.
17. Becke, A. D. *Phys. Rev. A* **1988**, 38, 3098–3100.
18. Lee, C.; Yang, W.; Parr, R. C. *Phys. Rev. B* **1988**, 37, 785–789.
19. Sprik, M.; Hutter, J.; Parrinello, M. J. *Chem. Phys.* **1996**, 105, 1142–1152.
20. Molteni, C.; Parrinello, M. J. *Am. Chem. Soc.* **1998**, 120, 2168–2171.
21. Trouiller, N.; Martins, J. L. *Phys. Rev. B* **1991**, 43, 1993–2006.
22. GAUSSIAN03, Gaussian, Inc., Wallingford, CT.
23. Root, D. F.; Saeman, J. F.; Harris, J. F. *Forest Prod. J.* **1959**, 158–165.
24. Harvey, J. M.; Symons, M. C. R.; Naftalin, R. J. *Nature* **1976**, 261, 435–436.
25. Harvey, J. M.; Symons, M. C. R. *J. Solut. Chem.* **1978**, 7, 571–585.
26. Bociek, S.; Franks, F. *J. Chem. Soc., Faraday Trans. 1* **1979**, 75, 262–270.
27. Collins, P. M.; Ferrier, R. J. *Monosaccharides*; John Wiley & Sons: New York, 1995.
28. Atalla, R. H.; Gast, J. C.; Sindorf, D. W.; Bartuska, V. J.; Maciel, G. E. *J. Am. Chem. Soc.* **1980**, 102, 3249–3251.
29. Earl, W. L.; VanderHart, D. L. *J. Am. Chem. Soc.* **1980**, 102, 3251–3252.
30. Atkins, P. W. *Physical Chemistry*; Oxford University Press: Oxford, 1986.